1

The Surface of Polymers

Rosica Mincheva and Jean-Marie Raquez

University of Mons (UMons), Laboratory of Polymeric and Composite Materials, Center of Innovation and Research in Materials and Polymers (CIRMAP), 20, Place du Parc, 7000 Mons, Belgium

1.1 Introduction

Surface properties of any polymers have an imminent influence over key properties such as wetting, adhesion, friction, and biocompatibility, therefore affecting the applicability of a polymer material [1]. It is nowadays well accepted that surface properties differ from bulk in many aspects and a multitude of scientific works has been done for the last 70 years in an attempt to highlight what actually constitutes the surface, including the interphase, and how far into the material its surface goes [2–10]. Moreover, while classical surface model will consider a surface as rigid, immobile, and at equilibrium, which is more likely to be true for rigid solids, the surface of a polymer material is highly depending on time and temperature due to its viscoelastic behavior and is therefore thermodynamically and kinetically dependent [11]. From this viewpoint , the polymer surface can continuously restructure and reorient in response to different external factors such as atmosphere, solvent, and so on and might be inherently a nonequilibrium dynamic system. The guiding force for these structural changes is that the surface tends to decrease its free energy in a continuous way. In other terms, surface chemistry, reactivity, and aspect vary in function of environmental and processing conditions, influencing any desired modification and/or application of the related material even when bulk properties are considered [12].

In order to understand the application-related modification of a polymer surface, one should first learn what the polymer surface is actually, how its properties are generally influenced, and what analytical methods are the most appropriate to study and understand. This chapter aims at providing a summary of experimental and theoretical concepts describing polymer surfaces near interfaces. It discusses the role of the different factors such as the surrounding environment in the surface properties and shows the multitude of analytical tools under different situations involving surfaces and interfaces.

Surface Modification of Polymers: Methods and Applications, First Edition.
Edited by Jean Pinson and Damien Thiry.

1.2 The Surface of Polymers

1.2.1 Definition of a Polymer Surface

The word "surface" in its most general use includes the outermost or the uppermost layer/boundary of a physical object or space/area (http://www.wordreference.com/definition/surface). From the materials science viewpoint, the surface, defined as the frontier between two different media, is characterized by a certain thickness, reflecting a gradient of properties. With this respect, surface ever differs from the bulk of any material in terms of density, composition, or structure, and, even if it is present at very small fraction (by comparison to bulk), the surface governs any polymer properties, as being the first contact sets on. This statement remains true whatever the macroscopic material, including polycrystalline solids or polymers.

However, for polymer surfaces, the molecular length scale goes well above the angstrom scale (e.g. a typical end-to-end distance is about 10^{-6} m for a polymer of 10 000 monomer units and considering the random-coil conformation [13]), and the term "small fraction" is broadly true. Herein, the connectivity, the entanglements and the interactions between polymer chains at the surface are built up for a surface thickness varying from several nanometers (for a layer in direct contact with other medium) up to several micrometers (for a crystalline morphology) [12]. Even though the interactions decrease upon increasing the distance, they remain the source of cohesion and determine the surface properties such as friction, adhesion, surface tension, and biological activity. Moreover, polymer chains have high degree of freedom (side-group [methyl, hydroxyl, carbonyl, etc.] C–C rotation, segmental α-process, and overall chain dynamics) and actual time and temperature-dependent local or long-range motions, making surfaces dynamic objects thereof [14] undergoing rearrangements upon changes into the surrounding phase(s): gas(es), liquid(s), or solid(s). Additionally, for a polymer macromolecule in the bulk, the interactions are similar in terms of type and force in all three directions, while for a macromolecule at the surface, they are unbalanced, leading to an excess of surface/interface free energy [15]. All these characteristics create a thermodynamic force (configurational entropy) – the guiding force determining an equilibrium state of minimal free energy or of maximum entropy by transferring end-groups, functional groups, or additives to the surface, which on the other hand causes segregation of polymer chains and/or their parts [5, 12]. The phenomena are known since the 70th of the twentieth century [16] and are emphasized even today [17]. Examples can be found for gels (presenting low or high contact angle in contact with water or air, respectively [18]), grafted polymers (where the grafted chains are found to be hidden in the bulk or exposed on the surface depending on the treatment conditions [19]), or even segmented polymers [16].

Consequently, a polymer surface is a dynamic surface having temperature and environmental responses – a place where phenomena provoking major evolutions influence the polymer properties and lifetime (Figure 1.1) [12, 20].

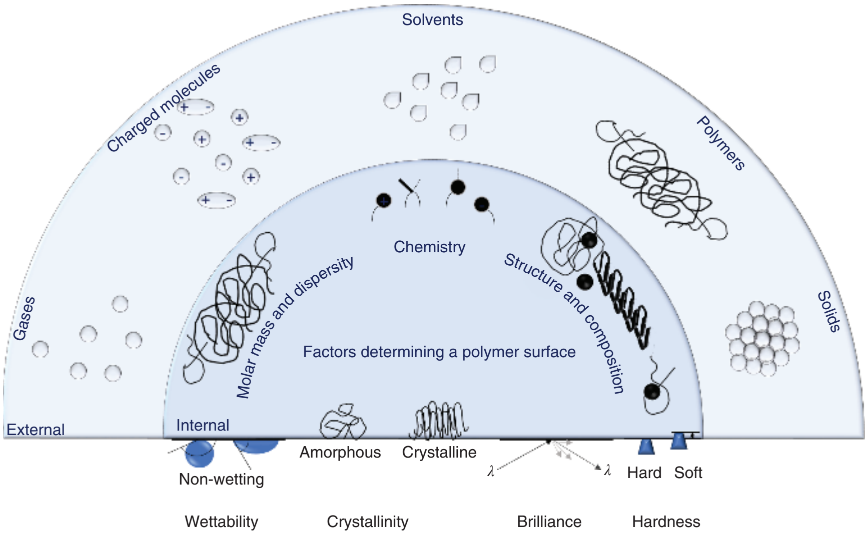

Figure 1.1 Schematic representation of factors determining a polymer surface and its related properties.

1.2.2 Factors Determining a Polymer Surface

The previously driven consideration suggests that the polymer surface will be determined by a multitude of factors within complex relationship without a sharp discrepancy between them. A very general classification, however, can be done based on factors' origin: (i) internal – related to the polymer itself and (ii) external – environment related.

1.2.2.1 Internal Factors

Among the internal factors, the polymer chemistry, composition and structure, and molar mass and dispersity can be listed:

Polymer Chemistry It is generally considered that aliphatic C—C or C—O bonds with non-bulky substituents are quite mobile and flexible, which make them able to adopt any infinite number of configurations (in the ideal case) with quasi-equal energy and to have a maximum entropy at thermodynamic equilibrium. In this case, the substituents will be exposed to the surface or not depending on the environment as shown by Cimatu et al. [21] for substituted (in terms of ethyl/methyl groups) polymethacrylates with hydroxyl, chloro, or phenoxy moieties. On the other hand, cyclic aliphatic or aromatic structures, branches, or cross-linking points, as bulky substituents have a marked stiffening effect that forces polymer chains to adopt a certain configuration that will reduce system entropy and increase free energy [22]. Bulky substituents will therefore be segregated at the surface [23], as illustrated by the studies of Hirai et al. [24] on polymethacrylates with "side crystalline" chains. Restrictive chain mobility and conformation are also related with the presence of functionalities allowing attractive hydrogen, dipole, or electrostatic interactions. Such functionalities will force adopting a certain conformation out of thermodynamic equilibrium. In other words, chemistry determines mobility and the properties of a dynamic polymer surface such as surface topography (or roughness) from atomic to macroscopic scale and surface morphology in terms of crystallinity and crystal structure [12, 13, 25]. Together, polymer chemistry, mobility, and conformation will influence the surface chemistry and thus the surface topography and wetting. Therefore, they all will play on surface mechanical properties, adhesion, friction, etc.

Polymer Composition and Structure Additives in polymers, especially of low molar mass (e.g. plasticizers), are often excluded from polymer bulk and migrate to the surface, changing its properties and composition [2]. Moreover, the composition will change with thickness and form a gradient. This is similar in the case of immiscible polymer blends, where the blend component with lower surface free energy will migrate to the polymer surface in order to reduce the total free energy of the system and place it in a thermodynamic equilibrium. Surface excess and concentration gradient can be calculated based on the mean field arguments [26, 27].

A similar effect is observed with block copolymers or comb-type copolymers where one sequence enriches the surface depending on miscibility and composition. In some particular cases, such segregation may even lead to the formation of lamellar structure normal to the surface [2].

Molar Mass and Dispersity Other important factors influencing polymer surfaces are polymer molar mass and dispersity [22]. A low molar mass polymer or a polymer with large dispersity, for example, is expected to present a greater number of chain ends at the polymer surface, when comparing with a high molar mass polymer or a polymer of lower dispersity. As chain ends are less restrained, they provide the polymer surface with greater mobility at low temperature, yielding it to expand. Greater mobility, as discussed earlier, will decrease surface free energy and affect topography and morphology.

Higher molar mass and lower dispersity, on the other hand, will cause entanglements and even some crystallization at the polymer surface. These will reduce chain mobility and increase surface free energy, causing irreversible topography and morphology changes.

1.2.2.2 External Factors

Understanding the interactions of polymer surfaces with external factors is important for selecting the right application. A multitude of examples can be found in areas of wetting and dewetting, crystallization, or “smart” materials for optoelectronics, as summarized in a very recent review [6]. Here again, the surface properties are thermodynamically driven in such a way to decrease the energy between different interacting components. This thermodynamically driven decrease in surface free energy is directly related to the dispersion forces, providing principal contribution to molecular interactions across polymer surfaces and allowing adsorption of substances from the environment (gas, liquid, or solid low- or high-molar mass molecules) to the polymer surface [12, 28, 29].

As shown by several reviews and experimental papers, these substances can also penetrate the surface and cause swelling or plasticizing at the near-surface regions [6, 8, 12, 29–31].

Gas Molecules Experiments on the physical adsorption of gases are one source of information about dispersion forces at interfaces [28]. They date back to the late 50–60th of the twentieth century and usually show a fast way to reach the adsorption equilibrium without any hysteresis, suggesting a lack of gas molecules penetration into the near-polymer surface range for energetically homogenic polymer surfaces [32]. Gas molecules penetration into the near-polymer surface range was found highly heterogeneous in terms of energetics polymer surfaces [29, 33], and it evidenced the contribution of the dispersion forces to the surface free energy. In these cases, a first gas monolayer is formed over the high energy portion of the adsorbent, followed by a second monolayer formation over the polymer surface [29]. More recent studies have shown that adsorption of gas molecules expanses polymer surfaces and causes plasticization of the near surface regions [12].

Charged Molecules The role of the dispersion forces should also be considered in the specific adsorption of ionic molecules onto polymer surfaces as it influences phenomena as conformation and solubility of electrolytes, flocculation, micelle formation, etc. [34]. For example, charged molecules such as salts and ionic surfactants, can form charged polymer surfaces from polymers that lack surface potential [8, 35]. The surface potential will be different from zero whether ions of the same sign are preferably adsorbed or equal to zero in the case of charge non-specific adsorption. This is due to the formation of an electrical double layer at the interface with a polymer surface of zero "native" surface potential as shown by the studies of Jacobasch et al. [35] on technical poly(ether ether ketone) (PEEK, Victrex 450G, Victrex GmbH, Germany) and a fluorocarbon polymer (provided by the Institute for Applied Polymer Research, Teltow, Germany). Indeed, these two polymers do have a zero "native" surface potential in aqueous solutions, because they do not contain dissociable surface groups. However, direct force and zeta potential experiments show a negative electrostatic surface potential due to an excess adsorption of anions from the electrolyte solution. Therefore, an electrical double layer is formed next to the solid polymer surface [35].

Such formation of an electrical double layer can be explained by considering the contribution of dispersion interactions acting on ions in the theory of colloid science. Specific ion adsorption due to dispersion interactions can be dominant as well as in the case of charged interfaces at high salt concentrations. The effect is shown to be at the same level of approximation as, and precisely equivalent to, the Onsager limiting law for the interfacial tension change related with dissolved salt at a single interface, i.e. to linearization of the Poisson–Boltzmann distribution, and restriction to electrostatic potentials as the sole determinant of adsorption excesses [8, 35].

Solvents Contact with solvents strongly influences polymer surface formation and restructuring, in terms of segregation, composition, and morphology [6, 31]. The comprehension of the mechanisms again lies on a consideration of thermodynamics. Polymers in contact with solvents tend to change conformation and configuration in order to reduce surface energy through the formation of temporary and favorable polymer–solvent interactions [6]. This ability of polymer surfaces to change their performance (actuate and interact) with the environment without requiring an external intervention conveys them as a form of a “smart” behavior that attracts a lot of attention.

The first studies in this aspect were based on conformational changes of polymer brushes induced by the environment [36]. Furthermore, they were translated to the migration of substituents and related to surface entropy and free energy [21, 22]. Hydrogen bonding, van der Waals interactions, or electrostatics were found to be responsible for solvent–polymer interactions. Complexity arises if solvent also lowers its free energy in contact with polymers. Therefore, solvent–polymer, solvent–solvent, and polymer–polymer interactions must be considered to understand how solvent influences polymer surface.

Solvent effects on polymer surfaces have been pioneered by Thomas and O’Malley [37]. The authors investigated the role of solvent–polymer interactions onto the surface chemical composition of thin poly(styrene)-*b*-poly(ethylene oxide) films. Results with different solvents showed that polymer surface enriches in the component allowing lowering the surface energy depending on solvent polarity, as expected from thermodynamics and energetics [37]. Additionally, and as expected from solubility considerations, a good solvent yielded less surface segregation of the soluble component, while a mutual solvent resulted in most pronounced composition-depth gradient. In other words, good solvent brings higher mobility of the polymer chains and reduces surface segregation due to preferential solubility and higher mobility [37]. On the opposite, a bad solvent contracts the polymer chains, restricts their motion, and favors surface segregation.

The picture becomes more complicated by introducing solvent–solvent to solvent–polymer interactions. For mixed solvents with preferential solubility to both components, highly segregated surfaces have to be obtained [38]. In this case, the effect of solvent–solvent interactions on polymer surface segregation was found predictable based on the Hildebrand solvent parameter and was considered relevant to solvent volatility [31]. Indeed, high solvent volatility decreases segregation by allowing less time for the process to occur.

Concerning polymer blends (polymer–polymer interactions) and the Hildebrand and Hansen solubility parameters, hydrogen (or electrostatic) bonding might be concluded to influence the phase behavior of polymer blends [39]. For miscibility based on hydrogen bonding polymers blends, a solvent of strong hydrogen bonding ability will reduce miscibility and induce segregation of polymer chains, based on competitive phenomena – solvation phenomenon (according to Horn [40]). This will be different from the behavior of immiscible polymer blends, where the surface organization is dominated by the equilibrium thermodynamics [31]. As already discussed, equilibrium thermodynamics favors complete phase separation and surface segregation of the component with lower surface energy [5, 12].

Lowering surface free energy might have undesired effect on polymer surface stability and gives rise to solvent absorption into the polymer and/or the dissolution of polymer into the solvent. These considerations have been investigated by Ruckenstein and Gourisankar [30], by a simple contact angle procedure for the case of polymeric surface water interface. The experiments were performed on three types of polymeric surfaces presenting high (Teflon FEP), medium (sputtered Teflon), and low (etched-sputtered Teflon) interfacial free energies with water as a result of surface restructuring in aqueous environment. The results from contact angle and dynamics of solid surface restructuring investigations under water evidenced the instability of polymer surface in the case of very small water–polymer interfacial free energy (the etched-sputtered solid surface), allowing penetration of water molecules from the surface to the bulk of the polymer material and possible dissolution of the solid in water. These contact angle results were well supported by the physicochemical characteristics of the different polymer surfaces used in this study [30].

The experimental works have been supported by a growing body of theoretical studies with the interest in switchable wettability and adhesion, mainly for polymer brushes in different geometries [41–46].

Polymers Another very intriguing (in view of applications) subject concerns the changes of a polymer surface when placed in contact with another polymer surface. Indeed, the idea of using polymer blends in order to broaden material applications is quite natural but turns out to be quite difficult. The reason for this comes from the competition between entropy and enthalpy, often guiding a phase separation of the pure polymers. The studies here lie on the Flory–Huggins theory of mixing and consider four potential sources of errors coming from the following assumptions:

- The long-range chain statistics of polymer molecules are ideal random coils, while in reality they might collapse in contact with another polymer [47].
- Large composition fluctuation should be neglected, although in the case of diluted regime or of low molar mass polymers, this mean-field theory faces a failure [48]. In the case of the dilute regime, the failure will be determined by the chain connectivity, while for low molar mass polymers, it will be induced by the absence of screening effects [4].
- There is no volume change (extra space creation) when two polymers are mixed. However, if two polymers are facing strong unfavorable interactions, such as repulsive forces, the system will tend to slightly lower density, reduce the number of possible interaction points, and gain some extra translational entropy in order to reduce energy. These all will create “vacancies” or extra space [4].
- There is now influence of the local structure and packing. Yet, it was already shown that bulky side groups or local structure of monomer units restrict the number of available conformations and thus provoke changes in entropy of mixing [4, 21, 23].

A large number of studies have gone into achieving universal theory, but with no success [4, 10, 49–51], and despite all its shortcomings, the Flory–Huggins theory (Eq. (1.1)) remains up to date the universal framework for considering polymer blends.

$$\chi = z(2\varepsilon_{\mathrm{AB}} - \varepsilon_{\mathrm{AA}} - \varepsilon_{\mathrm{BB}})/(kT) \tag{1.1}$$

where χ is the Flory–Huggins free energy of mixing, z – the z spatial dimension, $\varepsilon_{\mathrm{AB}}$, $\varepsilon_{\mathrm{AA}}$, and $\varepsilon_{\mathrm{BB}}$ – the energies associated to the interactions between neighboring segments: an A next to a B, an A next to an A, and B next to a B, respectively; k – the Boltzmann's constant ($1.380\,649 \times 10^{-23}$ J/K), and T – temperature (K).

According to this theory, polymer blends might be divided into three general classes:

- *Miscible polymer blends.* Occurring only in few cases, where the energy difference (χ, Flory–Huggins free energy of mixing) is negative, so intimate mixing between the components can be obtained [4]. Moreover, χ will be negative only for a certain temperature range, as shown for the case of deuterated poly(styrene)/hydrogenated poly(vinyl methyl ether) blends [52], and only within this temperature range, both polymers will be miscible for all molecular weights.
- *Similar polymer pairs.* Nearly identical in structure (e.g. differing only in isotropic substitution), where very small positive values of χ can be obtained. The classical example in this case is blends made of hydrogenated and deuterated components of equivalent structure [53]. Although the technological interest of such blends is irrelevant, they remain important for purely scientific studies of miscibility.
- *Immiscible polymer blends.* Comprising almost all other polymer blends lacking chemical similarity or specific interactions, where χ is taking a positive sign in the range 0.001–0.1 and both components will be miscible only for lowest molar masses [4].

Following the discussion, one may conclude that the important length scale for polymer–polymer interfaces is the overall size of the polymer chain, which broadens polymer/polymer interfaces compared with other liquids. Indeed, the width of polymer/polymer interface depends on polymer miscibility, and for miscible polymers the interface will broaden with time by the process of interdiffusion of polymer chains and result into a single phase at equilibrium [4]. This interdiffusion will be slow due to chain entanglements but will control the strength of the final material at equilibrium. On the opposite, immiscible polymer blends will tend to demix with time and will form coarsen domains at equilibrium (Figure 1.2). The predominant feature here being segregation with the lowest free energy component situated at the near-interface polymer surface [4].

Although, the knowledge on how polymer molecules orient and interact with the molecules of another polymer at the interface, the subject continuously evokes interest as shown in the significant number of scientific papers, reviews, book chapters, and books on polymer blends in the very recent years [55–73].

Solid Surfaces As was shown earlier, the composition of a polymer surface in contact with a small molecule or with another polymer significantly differs from bulk. The same applies to the polymer surface in contact with a solid and is of

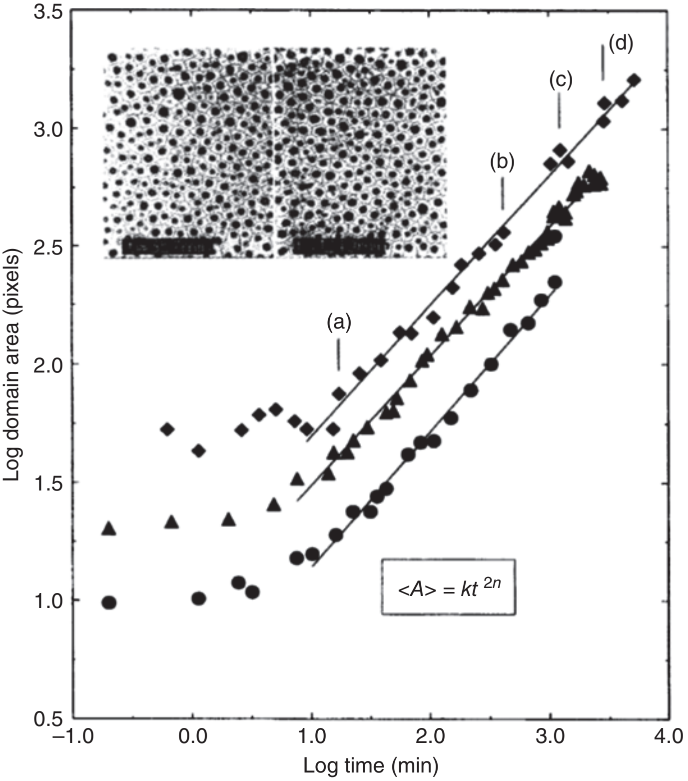

Figure 1.2 Domain coarsening. Temporal domain area <A> for three runs at a defined composition and temperature. "k" – rate of growth of the mean radius, "n" – the exponent in the growth low and "t" – growth time. Solid lines represent linear fits and (a) – (d) are optimal parameters obtained from Gaussian fits. Inset: snapshots of domain patterns at different stages of coarsening (from the top plot); the black panels correspond to 150 μm (left) and to 240 μm (right). Source: Seul et al. 1994 [54]. Reused with permission from Scientific Publishing and Remittance Integration Services.

importance in a number of problems of practical interest as polymer processing, lubrication, permeation, separation, and adsorption processes [74–77]. A very practical example can be found in colloid and surface science, where the polymer surface will respond to a solid colloid particle by either preventing or enhancing its aggregation, depending on polymer-induced phenomena, known as adsorption or depletion [77]. Basically, both these terms refer again to the surface segregation or enrichment in the species of low surface energy at contact. As already discussed for other factors, large degrees of adsorption or segregation can be obtained even when the interaction driving the segregation is small; offset against any gain in energy obtained on adsorption is a loss of translational entropy of the molecule in the bulk, but for a large macromolecule this entropy is rather small. The length scale characterizing the distance from the surface over which the composition is perturbed is generally much larger than that for small molecules, either liquid or solid, because this length scale is itself set by the size of the molecules themselves [4].

The difficulty to understand the behavior of polymer chains at solid interfaces comes from the fact that there are inaccessible (buried). According to the literature, the polymer/solid interface structure is determined by the molecular interactions at such buried interfaces [78–82]. Therefore, elucidation of interfacial structures at the buried polymer/solid interface leads to the detailed understanding of the buried interfacial interactions, which can be used to rationally design interfacial structures with improved properties (e.g. adhesion). According to the chemistry of the solid, polymer/solid interfaces might be divided into three main groups: polymer/metal, polymer/metal oxide and polymer/polymer interfaces. The later has been shortly discussed earlier, so this section will focus on the behavior of polymer chains in contact with metal and metal oxide surfaces.

- *Polymer/metal interfaces* have been studied [78] due to their importance in microelectronics or anticorrosion coating applications, with one of the largely investigated model systems being the poly(methyl methacrylate) (PMMA)/silver (Ag) interface. Experiments have shown that at this buried interface, in addition to the surface dominating ester methyl groups of PMMA, the methylene groups and the alpha methyl groups are also present. Orientation analysis indicated that the side ester methyl groups at the PMMA/Ag interface tilted toward the polymer/metal interface [83]. Using a self-assembled monolayer of methyl 3-mercaptopropionate (MMP) on Ag as a control, the absolute orientation of ester methyl groups of PMMA at the buried PMMA/Ag interface was deduced to be tilting away from the Ag surface (Figure 1.3) [84].

Last experiments studied the interfacial molecular structures of an adhesion promoter, polybutadiene modified epoxy (PBME) rubber or polystyrene (PS), with gold (Au) [85, 86]. Buried surfaces of perfluorosulfonated ionomers (such as Nafion), used in fuel cells and electrodes (such as Pt) have also been investigated [87]. The obtained results suggested that Nafion molecules interact with the Pt electrode surface via side-chain sulfonate terminals. Besides the evolution of polymer chemical functionality in contact with metal surfaces, the conformation evolution of the macromolecules was also investigated [80]. For PS chains at the surface of a spin-coated film in a temperature-ramping mode as well as under isothermal annealing, the conformation of the surface chains was

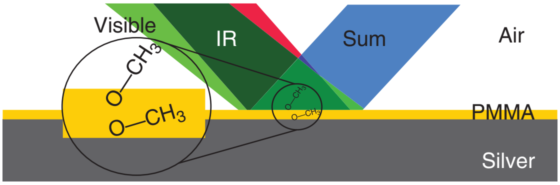

Figure 1.3 Molecular structure of the buried PMMA/Ag interface studied by Sum frequency generation (SFG) vibrational spectroscopy showing side ester methyl groups tilting toward the polymer–metal interface. Source: Adapted with permission from Lu et al. [83]. Copyright 2018, American Chemical Society.

found to be in a nonequilibrium state. Based on these studies, the relaxation of surface nonequilibrium chains was stated to be induced by the enhanced surface mobility, while the whole chain motion (such as reptation) was suggested to be a key factor in determining the time scale for equilibrating the surface chain conformation [80].

- The importance of *polymer/metal oxide interfaces* can be found in the use of metal oxides (such as SiO_2) as (nano)fillers in polymer (nano)composite materials to enhance the mechanical strength of the final material. The multitude of experimental and theoretical (modeling) studies have pointed out the importance of polymer/filler interactions (such as hydrogen bonding or CH–π) and the preparation method (spin- or solvent-casting) onto the chemical and conformational structure of the polymer chains ate the interface [78, 88, 89].

More detailed information on the conformation of the polymer chains near interfaces can be found in the late literature, summarized in the book of Jones et al. [4]

1.2.3 The Polymer Surface at a Microscopic Level

An elegant physical argument about the effect of a surface on polymer configurations was made by Silberberg in 1982, who argued the conformational modifications by considering an imaginary plane cutting a polymer melt in an exact mirror image [90]. In particular, each configuration that crosses the plane has an image configuration crossing in the other direction. Moreover, if cutting each chain that crosses the plane and joining up the free end with the cut end of the mirror conformation, there remain no bonds crossing the plane, but the same number of bonds are still present. From this, these chains whose centers of gravity lie less than about two radii of gyration from the surface will have their configurations perturbed; in particular the radius of gyration perpendicular to the interface will tend to be reduced, with rather less change occurring in the directions in the plane of the surface [90].

This picture of chains near the surface adopting rather flattened configurations has been confirmed by lattice Monte Carlo study in computer simulations, considering the position of the chains, the chain-monomer profile (as the average number of monomers in a layer a given distance z from the surface that belong to the same chain), and the location of the chain ends [91]. Simulations herein confirmed the hypothesis (based on physical grounds) that a polymer chain at or near an interface suffers from a smaller loss of entropy (by virtue of the surface) than does a chain with a middle segment at the surface, so that the density of chain ends at the surface should be somewhat enhanced.

The knowledge over polymer interactions and chain conformation in contact with surfaces is extremely important in the construction of materials for healthcare applications [92]. Studies in this field consider mainly protein orientation (in terms of chemical functions and chain conformation) at the contact with other surfaces. Despite any difference, they might be translated to any other polymer chain and shed much light on the subject of what a polymer surface is.

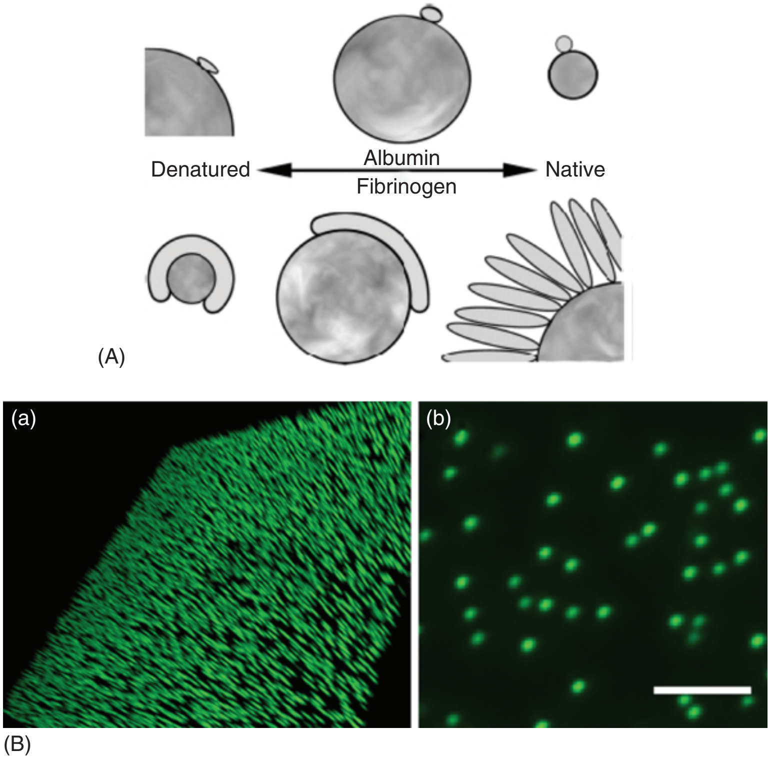

Figure 1.4 Schematic representation demonstrating control of conformation and orientation by surface curvature (A) (Source: Reproduced with permission from Giamblanco et al. [97]. Copyright 2018, American Chemical Society) and (B) laminin adsorbed on a GaP nanowire substrate (Source: Reproduced with permission from Fortes [99]. Copyright 1983, Springer Nature). Confocal three-dimensional stack image of a 143 × 143 μm^2 area with vertical 90 μm diameter, 3.2 μm long GaP nanowires (a). Single plane image (7.3 nm optical slice) of the same sample (b). Scale bar 3 nm [99].

Based on a considerable body of experimental and theoretical work, the orientation of a protein molecule on the surface can be characterized as “side on” or “end-on” depending on the axis (long or short, respectively) interacting with the surface [93–98]. Such interactions have been found to strongly influence the protein secondary structure. Another important factor is the surface curvature. High surface curvature (as in the case of carbon nanotubes or silica nanoparticles) promotes globular structure [97], while flat surfaces (such as gallium phosphate) is more suitable for rod-like macromolecules (Figure 1.4) [99].

1.3 Properties of Polymer Surfaces at Interfaces

The dynamic nature of the structure and morphology of polymer surfaces near interfaces influences surface properties and fascinates scientists since more than half a century. Among all, surface wettability, density, adhesion, thermal (surface glass-transition temperature and crystallinity), optical (brilliance), and mechanical (surface modulus, flexibility) properties are of primary interest in terms of applications.

1.3.1 Surface Wettability

Historically speaking, the first surface property to be studied is the surface wettability, defined as the ability of a material to remain solvated in the presence of other molecules. The more common situation in wetting involves a solid (s), interacting with a liquid (l), at the environment of a second immiscible fluid (v) [100], each of them characterized by its interfacial tension under equilibrium conditions at a certain temperature (γ_{sv}, γ_{sl}, and γ_{lv}, respectively). From a physical point of view, the phenomenon is explained by the cohesive forces holding liquid molecules together determining surface tension. As polymer macromolecules at the surface are also held together by the action of cohesive forces, they undoubtedly exhibit surface tension. Detailed consideration and understanding of this phenomenon with polymers are present in the books of Fortes [99] and Jones et al. [4] and recently reviewed by Hall and Geoghegan [6], and therefore this part of the chapter will only aim on providing a picture of the influence over the internal and external factors discussed earlier on surface wettability in terms of surface tension.

Surface tension is calculated from contact angle (θ, °) measurements and compared to water. With this respect surfaces are divided into hydrophilic (where the interfacial energy at the water–polymer surface contact is below the free surface energy of the polymer) and hydrophobic (where the polymer surface is of lower free energy compared with the interfacial energy at the water–polymer interface). If θ is constant with time and the surface is in equilibrium, it will be expressed by the Young's equation (1.2)

$$\theta = \arccos\left(\frac{\gamma_{\text{sv}} - \gamma_{\text{sl}}}{\gamma_{\text{lv}}}\right) \tag{1.2}$$

where the surface free energies are assumed to have the same value at all points in each interface [100, 101]. This equation is only true for the case of ideal surface (unreactive and chemically homogeneous, insoluble, completely flat, rigid, and static) [6]. From the already exposed definition, however, polymer surfaces are dynamically changing objects, responsive to internal and external stimuli. This dynamic nature creates instability in the contact angles, described by a contact angle hysteresis – a change in a droplet shape and volume provoked by spreading and/or adsorption. In practice, the dynamic phenomenon of contact angle is limited between the advancing (maximal) contact angle (θ^{adv}) and the receding (minimal) contact angle (θ^{rec}), the first associated to wetting and the second to dewetting of a surface [102]. The picture might be visualized according to Figure 1.5.

It is then natural to consider that internal factors such as polymer chemistry (presence of reactive/functional groups along the chains, lateral, or chain ends), composition (presence of additives), and dispersity (presence of low molar mass chains) will influence surface reactivity, chemical homogeneity, and

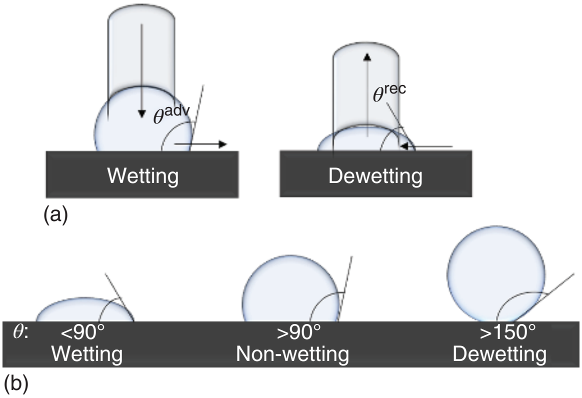

Figure 1.5 Schematic representation of the wetting and dewetting of a surface (a) and according to the contact angle value (b). "*θ*" - contact angle.

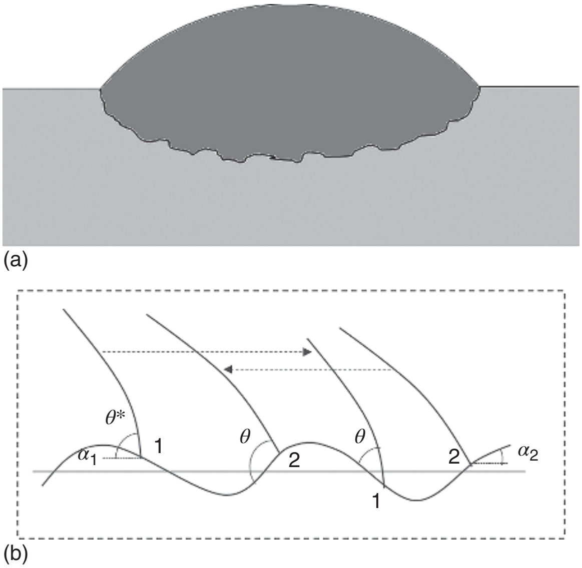

Figure 1.6 Schematic representation of (a) the "beer bottle cap" concept and (b) of a profile of rough surface showing the expected critical positions of the contact line for the advancing (1) and receiving (2) modes. The line of contact jumps (arrows) between the positions indicated as the volume of the drop is made to change. The horizontal line represents the mean surface. Source: Fortes et al. 1983 [99]. Adapted with permission of Springer Nature.

solubility [100]. External factors such as gases, solvents, polymer, and solids will change the hydrophilic/hydrophobic balance due to the thermodynamically driven reorganization of the functional groups exposed at a polymer surface [6, 31]. This creates a multiplicity of equilibrium configurations of polymer chains near the surface and consequently modifies surface wettability. This multiplicity of equilibrium configurations is expected to give rise to a waved contact lines between polymer surface and a liquid drop and to a liquid interface with convolutions near the polymer surface as described by the "beer bottle cap" concept (Figure 1.6a) [100]. Reconstructuring due to conformational changes (chain motions as displacement and reptation) will induce local variations in surface rugosity and rigidity that will create a droplet spreading and/or adsorption. It is obvious that modifications in surface roughness also induces the previously discussed multiplicity of equilibrium configurations for polymer chains near the surface and thus influences surface wettability. The effect can be explained with Figure 1.6b, where the observed contact angle, measured in relation to the mean surface (θ^*) is actually the sum of the real θ and α_1 at point 1 or the difference between θ and α_2 at point 2 [100].

Practically, surface wetting is an indicator of surface fouling and adsorption for example in protein fouling. Here, two cases can be observed:

- In the case of hydrophilic polymer surfaces, the strong surface wettability creates a high-density layer of adsorbed water molecules that shields the polymer surface and prevents it from interactions with proteins [92]. In this case, surfaces are characterized with limited (if any) protein fouling as very limited (if any) polymer–protein interactions are possible and proteins preserve their secondary structure.
- On the opposite, proteins undergo partial unfolding and spreading onto hydrophobic surfaces, where polymer–protein interactions are highly possible. Decreasing fouling of such hydrophobic surfaces is then possible with introducing specific nanocharges, influencing the morphology and the rugosity of the polymer surface at the nano-level [17, 103]. Similar results are obtained with polymer surfaces when wetting with nonaqueous solvents.

Thus, the surface reorganization upon wetting is an extremely important factor to be taken under consideration when choosing the right application of a polymer material.

1.3.2 Surface Thermal Properties

If it is intuitive to think that polymer chains near the surface would have higher degree of freedom, and thus higher mobility in comparison to bulk ones [12], it is also intuitive to consider that the thermal properties – glass (T_g) and melting (T_m) transition temperatures and crystallinity – will also differ from bulk. These hypotheses are confirmed by experimental works showing the importance of the environment (external factors) on chain mobility and thus on chain orientation and rearrangement [8]. Experiments also revealed gradient evolution of polymer thermal properties from surface to a bulk [104]. In general, there are three factors to be considered to determine mobility and consequently thermal properties of polymers: chain flexibility, interchain interactions, and polymer regularity [22], all of them determined by internal (polymer chemistry, composition, and molar mass) or external (contact with gas, solvent, or solid) factors. The way that they influence bulk transition temperatures and crystallinity was recently described by Gilbert [22] and can easily be transferred to the polymer chains near the surface.

1.3.2.1 Surface T_g

For a polymer surface *below the glass transition temperature* (T_g), where molecular rotation about a single (C—C) bond becomes restricted and where the backbone dynamic is completely frozen, only small side-groups (methyl, hydroxyl, carbonyl or phenyl substituents) can move [105]. It is then clear how polymer chemistry, composition, and molar mass will influence T_g.

- In terms of *polymer chemistry*, the presence of more bulky substituents will restrict local motions from rotation to torsional processes, flips, or only oscillations and thus increase surface T_g. The presence of polar or hydrogen bonding groups will also tend to increase T_g, as they might create bonding between adjacent groups and thus increase the energy required for side-groups movement.
- In terms of *composition*, branching with long side-chains or cross-linking will cause entanglements and again rise the T_g.
- A low *molar mass* polymer will have higher amount of chain ends tending to migrate to the surface and increase its mobility, which reduces T_g. The relation between T_g and the number average molar mass of ($\overline{M}_n$) a polymer is given by the Flory–Fox equation (1.3):

$$T_g = T_g^{\infty} - \left(\frac{K}{\overline{M}_n} \right) \tag{1.3}$$

where T_g^{∞} is the glass transition temperature of a sample containing polymer chains of infinite molar mass and K is a positive constant [106].

Above T_g, segmental relaxation (α-relaxation) process, based on cooperative motion of chain segments, completes side-group dynamics. Here, the rotation of one part of the macromolecule about another one (over a C—C or C—O bond) will also be impeded by the presence of more bulky groups (hydrocarbon groups, phenyl groups, etc.) along the polymer chain backbone and T_g will increase again [22]. The presence of unsaturations as double (C=C) or triple bonds (C≡C) will stiffen the chain at the point of inclusion but might increase the flexibility of adjacent bonds, thus reducing the overall glass transition temperature. If polymer composition is concerned, random copolymers will have a T_g between those of the corresponding copolymers according to the Fox equation (1.4):

$$\frac{1}{T_g^{\mathrm{mix}}} \approx \sum_i \frac{\omega_i}{T_{g,i}} \tag{1.4}$$

where T_g^{mix} and $T_{g,i}$ are the glass transition temperature of the mixture and of the component i and ω_i is the mass fraction of component i [107]. It must be pointed out that since random copolymerization tends to promote disorder and reduce molecular packing and interchain interactions, the T_g of random copolymers is often lower (although sometimes also higher) than predicted by the linear relationship. In the case of block copolymers, two types of effect have been observed depending on blocks miscibility/compatibility. For incompatible sequences, a transition corresponding to each block is observable, while for compatible blocks a single transition is observed. This last one is also usually close as predicted by the linear relationship [22].

Both below and above bulk T_g, *external factors* as the presence of gases, liquids, or solids will generally cause chain separation and increase mobility [22, 105]. This effect is known as plasticization and results in a shift of the surface T_g toward lower temperatures with respect to bulk T_g. As an example, the system poly(methyl phenyl siloxane) (PMPS)/organophilized silicate might be cited [105]. With this system, a very fast process was found to dominate the dielectric spectra with a very weak, almost Arrhenius temperature dependence. Additionally, at high temperatures its dynamics appeared to overlay the dynamics of the bulk PMPS, whereas near and even below the bulk T_g, it was almost 6 orders of magnitude faster than the bulk segmental process. The attempt to analyze the relaxation times of this process resulted in a Vogel temperature T_0 of about 93 ± 2 K, i.e. almost 100 K lower than that in the bulk. The fragility parameter, $D = B/T_0$ also increases about five times for the confined chains with comparison to the PMPS, indicating that the confined PMPS behaves as a stronger glass (more Arrhenius-like), i.e. confinement influences a conformational rearrangement. At high temperatures, a slow process was evident with a weak dielectric strength and its relaxation times coinciding with the ones of the bulk polymer; likely, this was due to the segmental motion of PMPS, which occurred outside the galleries of the nanocomposites. This is because the relaxation times of the polymer chains at the surface are much shorter than those of the bulk and follow almost Arrhenius temperature dependence [105]. Alternatively, the enhanced dynamics of surface polymer chains might be explained by an enhanced monomeric mobility due to preferential parallel organization of the polymer chains in contact with another surface that increases supercooling [108].

1.3.2.2 Surface Crystallization

In the case of semicrystalline polymers, their crystallization starts with the formation of lamellae [109, 110], due to chain folding effects. The lamellae grow at different rates (with the fastest rate dominating the crystallization) until spherulites are formed. Given this, crystallization is considered as a kinetic phenomenon, although some considerations of a spinodal process also exist [111].

Here again, among the *internal factors*, polymer chemistry plays an important role in crystallization as it determines chain regularity [22]. For bulk polymers, it is generally considered that regular polymers (with long linear chains) will be able to crystallize, while branched or cross-linked polymers will form amorphous structures. This somehow implies that polymer chains near the surface, where the concentration of branches and chain ends is much higher the bulk, impeding crystallinity. However, the higher mobility of polymer chains in the presence of branches and chain ends facilitates rearrangement and would eventually improve crystallization. Moreover, long branches can bring chain entanglements and even crystallization. Due to all these differences, the surface formed by polymer crystals might have different perfection (size and shape) and therefore, different melting/crystallization temperatures.

If not the most important, the most discussed *external factor* influencing the crystallization of polymer chains at surfaces is the solid surface related with nucleation [6, 22]. The role of a solid surface in polymer crystallization (epitaxy) is important, particularly because it is accepted that polymer crystallization proceeds by nucleation. In this case, the solid surface takes the role of a nucleating site for crystallization. This would mean that crystallization proceeds at a higher temperature on cooling or at a lower temperature on heating (if cold crystallization is involved) [6]. These hypotheses are confirmed by experimental results, mostly including poly(ethylene terephthalate) (PET) [112–114]. Results have shown that PET at a solid surface will start its surface crystallization at a temperature close to its glass transition temperature, i.e. below the bulk T_c occurs. Because of this faster crystallization at surfaces, the process is considered to be confinement controlled, what basically means that the thickness of the sample in contact with a solid surface will be another important factor in crystallization of surface polymer chains [114].

In any case, considering the overall thermal properties of a polymer surface is of crucial importance as it imminently influences surface optical and mechanical properties.

Surface Optical Properties Among the polymer material optical properties, the transparence and the brilliance are the most often sought in a multitude of industrial application areas such as painting, automobile, etc. Between them, the brilliance is the surface property that scientists and industry often focused on.

The brilliance translates the ability of a surface to reflect light, or its reflectance (R). This last one being defined as the ratio between the amount of reflected (Φ_e^r) and incident (Φ_e^i) light in a gas or fluid. Ideally, in air and on a plain surface R will be only dependent on the incident light angle and the refractive index of the material, which is determined by internal factors as surface chemistry (for polymer surfaces, surface chemistry). However, reaching this ideal case of plain surfaces is not always easy, and for the most common rough surfaces, the light is not only reflected but also diffused in the environment just above the surface (Eq. (1.5)):

$$R = R_0^{\frac{4\pi\sigma\cos\theta}{\lambda}} \tag{1.5}$$

where σ is the surface root mean squared roughness, θ is the incident light angle, and λ is the incident light wavenumber [115].

Surface Mechanical Properties Last, but not least, the mechanical properties of a polymer surface raise significant interest as they represent a direct measurement of the surface resistivity toward mechanical aggressions as abrasion. As surface thermal properties (T_g and crystallinity) were found to differ from bulk with a gradient evolution from the surface to the polymer bulk [8, 104, 105], the surface mechanical properties are also suggested to differ from these of the bulk [116]. Indeed, experimental studies have shown that surface dynamic storage modulus (E') and surface loss tangent (tan δ) vary as a function of polymer surface chemistry, polymer surface chains molar mass, segregation, and composition (enrichment in chain-end groups) [116]. Surface Young's modulus (E) and surface hardness (H) on the scale of 0.05–1 μm were also found to be related to polymer homogeneity at a surface [117], which is affected by the complex action of both internal and external factors. With similar experiments, the E variation with depth is also confirmed [118]. Despite the fact that the experiments provide direct information on the surface properties of polymers, their scientific knowledge requires the use of numerical simulation techniques [119].

Table 1.1 Analytical methods and general information for the characterization of polymer surfaces [2, 6, 11, 78, 119].

	Method	Radiation		Dept		Information			Surface
		In	Out	Resolution	Profiling	Chemistry	morphology	Typical	
	Contact angle (CA)			<1 nm				Wettability and surface tension	Accessible
	Quartz crystal microbalance with dissipation (QCM-D)			nm				Adsorption, adhesion, interactions, and reactions	Accessible
	Inverse gas chromatography (IGC)	Ar, N_2, CH_4						Local short-range motions and relaxations	Accessible
Spectroscopic	High resolution electron energy loss spectroscopy (HREELS)	e^-	e^-	1 nm		Yes		Vibrational spectrum	Accessible
	Static secondary ion mass spectroscopy (sSIMS)	Ions	Ions	1 nm		Yes		Surface chemistry	Accessible
	X-ray photoelectron spectroscopy (XPS)	X-ray	e^-	<5 nm	Yes	Yes		Surface chemistry	Accessible
	Electron spectroscopy for chemical analyses (ESCA)	X-ray	e^-	<5 nm	Yes	Yes		Surface chemistry	Accessible
	Infrared attenuated total reflection (IR-ATR)	Light	Light	μm	Yes	Yes		Vibrational spectrum	Accessible
	Nuclear magnetic relaxation (NMR)	^{13}C decoupling		T_1 and T_2	Yes	Yes		Chain and segment mobility	Accessible and buried
	Sum frequency generation surface vibrational (SFG)	Light	Light	nm	Yes	Yes		Vibrational spectrum	Accessible and buried
	Dynamic SIMS (dSIMS)	Ions	Ions	12	100 nm	Yes	Yes	Interface width/profile, chemistry	Buried
	X-ray scattering (XR)	X-ray	X-ray	0.2 nm	Yes	Yes	Yes	surface Chemistry, shape, and profile, roughness	Accessible

(Continued)

Table 1.1 (Continued)

Method		Radiation		Dept		Information			Surface
		In	Out	Resolution	Profiling	Chemistry	morphology	Typical	
Microscopic	Atom force microscopy (AFM)			0.1 nm		Yes	Yes	Topography, structure, chemistry, mechanical, and electrical properties	Accessible
	Phase measurement interference microscopy (PMIM)	Light	Light	0.6 nm			Yes	Roughness, homogeneity	Accessible
	Scanning tunneling microscopy (STM)		e^-	0.1 nm			Yes	Topography	Accessible
	Scanning electron microscopy (SEM)	e^-	e^-	>10 nm			Yes	Topography, structure	Accessible
	Transmission electron microscopy (TEM)	e^-	e^-	3 nm	100 nm		Yes	Interface width/profile	Buried
Ion-beam	Elastic recoil detection (ERD)	^{4}He	H, D	80 nm	100 nm		Yes	Interface width/profile	Buried
	Forward recoil spectroscopy (FRS)	^{4}He	H, D	80 nm	100 nm		Yes	Interface width/profile	Buried
	Rutherford back scattering (RBS)	^{4}He	^{4}He	30 nm	100 nm		Yes	Movement of markers	Buried
	Small angle X-ray scattering (SAXS)	X-ray	X-ray	1 nm	100 nm		Yes	Interface width/area	Buried
	Small angle neutron scattering (SANS)	No	No	1 nm	100 nm		Yes	Interface width	Buried
	Nuclear reaction analysis (NRA)	^{3}He, ^{15}N	^{4}He, γ	14, 30, 4, 12	@surface, 100 nm		Yes	Interface width/profile, element specific	Buried
	Neutron reflectometry (NR)	No	No	0.2 nm	100 nm		Yes	Interface width/profile	Buried
Infrared densitometry (IR-D)		Light	Light	10 μm	100 nm		Yes	Interface width/profile	Buried
Ellipsometry		Light	Light	0.2 nm	100 nm		Yes	Thickness	Buried
Surface plasmons		Light	Light	0.2 nm	100 nm		Yes	Thickness	Buried

1.4 Experimental Methods for Investigating Polymer Surfaces at Interfaces

The scientific knowledge on polymer surfaces at the interfaces will also depend on the analytical method of choice [2, 6]. In general, analyses must provide information on chemistry and chain conformation, chain-end distribution, surface density and roughness, etc. with sufficient resolution (sub-nanometer scale) [2]. Although the analytical methods allowing knowledge on the polymer surface near an interface are numerous nowadays, their choice is far from being trivial. Indeed, the choice of relevant technique will depend on several factors:

- What information (chemistry, morphology, etc.) is needed.
- What is the surface accessibility (e.g. the type of external factor = accessible and buried surfaces).
- What the required resolution is.
- Sample form in terms of preparation method.
- Is the sample to be destroyed or preserved.

Some techniques also allow depth profiling and give access to information on lateral structures [2]. Thus, analyses of polymer surfaces at interfaces are case specific. In the very recent review of Hall and Geoghegan [6], the available analytical methods for polymer surface characterization are split according to surface accessibility and discussed in details. Here, they are summarized in with some additional information in Table 1.1.

1.5 Conclusions

In this chapter, the polymer surface is described and defined as a dynamic surface with temperature and environmental responses. The influence of a multitude of internal (in terms of polymer chemistry, composition, and molar mass) and external (gas and solvent molecules, polymers, and solids) on polymer surface chemistry and organization is integrated based on literature data. Some basic thermodynamically controlled properties are also discussed in view of the temperature and environmental response of polymer surfaces. Finally, the available analytical methods for the characterization of polymer surfaces and the general information they can provide are listed.

References

1 Elbert, D.L. and Hubbell, J.A. (1996). Surface treatments of polymers for biocompatibility. *Annu. Rev. Mater. Sci.* 26: 365–394. https://doi.org/10.1146/annurev.ms.26.080196.002053.

2 Stamm, M. (1992). Polymer interfaces on a molecular scale: comparison of techniques and some examples. *Macromol. Synth. Order Adv. Prop.* 100: 357–400. https://doi.org/10.1007/BFb0051632.

3 Opdahl, A., Koffas, T.S., Amitay-Sadovsky, E. et al. (2004). Characterization of polymer surface structure and surface mechanical behaviour by sum frequency generation surface vibrational spectroscopy and atomic force microscopy. *J. Phys. Condens. Matter* 16 https://doi.org/10.1088/0953-8984/16/21/R02.

4 Jones, R.A.L., Richards, R.W., and Muthukumar, M. (2000). Polymers at surfaces and interfaces. *Phys. Today* 53: 59–59. https://doi.org/10.1063/1.1292488.

5 Lu, X., Zhang, C., Ulrich, N. et al. (2017). Studying polymer surfaces and interfaces with sum frequency generation vibrational spectroscopy. *Anal. Chem.* 89: 466–489. https://doi.org/10.1021/acs.analchem.6b04320.

6 Hall, A.R. and Geoghegan, M. (2018). Polymers and biopolymers at interfaces. *Rep. Prog. Phys.* 81 https://doi.org/10.1088/1361-6633/aa9e9c.

7 Schneider, K. (2008). Mechanical properties of polymers at surfaces and interfaces. *Polym. Surf. Interfaces*: 139–160. https://doi.org/10.1007/978-3-540-73864-0.

8 Garbassi, F., Morra, M., Occhiello, E., and Garbassi, F. (1998). *Polymer Surfaces: from Physics to Technology*. Chichester: Wiley.

9 Sanchez, I.C. (2013). *Physics of Polymer Surfaces and Interfaces*. https://books.google.fr/books?hl=fr&lr=&id=PU1HBQAAQBAJ&oi=fnd&pg=PP1&dq=Molecular+Interpretations+Polymer+Interface+and+Adhesion&ots=cWrbgBV44B&sig=o4znlrg9NlW1H-eYwf6Ulm4FIKY#v=onepage&q&f=false.

10 Koberstein, J.T. (2004). Molecular design of functional polymer surfaces. *J. Polym. Sci., Part B: Polym. Phys.* 42: 2942–2956. https://doi.org/10.1002/polb.20157.

11 Andrade, J.D. (ed) (1997). Polymer Surface Dynamics. https://doi.org/10.1016/S0166-2481(08)70652-4.

12 Darque-Ceretti, É., Felder, E., and Haudin, J.M. (2003). Introduction a l'etude et a l'analyse des surfaces et interfaces de polymeres. *Ann. Chim. Sci. Des Mater.* 28: 1–14. https://doi.org/10.1016/S0151-9107(03)00048-5.

13 Hill, R.G. (2005). *Biomaterials, Artificial Organs and Tissue Engineering*. Woodhead Publishing https://doi.org/10.1533/9781845690861.1.37.

14 Stamm, M. (2008). *Polymer Surfaces and Interfaces*. https://doi.org/10.1007/978-3-540-73865-7.

15 Bazaka, K. and Bazaka, O. (2015). Superhydrophobic polymers. In: *Superhydrophobic Surfaces*, 67–85. https://doi.org/10.1016/B978-0-12-801109-6.00005-7.

16 Sung, C.S. and Hu, C.B. (1979). Application of Auger electron spectroscopy for surface chemical analysis of Avcothane. *J. Biomed. Mater. Res.* 13: 45–55. https://doi.org/10.1002/jbm.820130107.

17 Beigbeder, A., Jeusette, M., Mincheva, R. et al. (2009). On the effect of carbon nanotubes on the wettability and surface morphology of hydrosilylation-curing silicone coatings. *J. Nanostruct. Polym. Nanocompos.* 5: 37–43.

18 Holly, F.J. and Refojo, M.F. (1975). Wettability of hydrogels I. Poly(2-hydroxyethyl methacrylate). *J. Biomed. Mater. Res.* 9: 315–326. https://doi.org/10.1002/jbm.820090307.

19 Ratner, B.D., Weathersby, P.K., Hoffman, A.S. et al. (1978). Radiation-grafted hydrogels for biomaterial applications as studied by the ESCA technique. *J. Appl. Polym. Sci.* 22: 643–664. https://doi.org/10.1002/app.1978.070220306.

20 Chen, Z.-F., Zhang, W., and Wang, X.-P. (2006). Advances in polymer surface reconstruction. *Polym. Mater. Sci. Eng.* 22: 6–9.

21 Cimatu, K.A., Chan, S.C., Jang, J.H., and Hafer, K. (2015). Preferential organization of methacrylate monomers and polymer thin films at the air interface using femtosecond sum frequency generation spectroscopy. *J. Phys. Chem. C* 119: 25327–25339. https://doi.org/10.1021/acs.jpcc.5b07688.

22 Gilbert, M. (2016). Relation of structure to thermal and mechanical properties. *Brydson's Plast. Mater. Eighth Ed.*: 59–73. https://doi.org/10.1016/B978-0-323-35824-8.00004-9.

23 Higaki, Y., Kobayashi, M., Hirai, T., and Takahara, A. (2018). Direct polymer brush grafting to polymer fibers and films by surface-initiated polymerization. *Polym. J.* 50: 101–108. https://doi.org/10.1038/pj.2017.61.

24 Hirai, T., Osumi, S., Ogawa, H. et al. (2014). Precise synthesis and surface wettability of a polymer with liquid crystalline side chains. *Macromolecules* 47: 4901–4907. https://doi.org/10.1021/ma5010265.

25 Meng, Q., Honda, S., Tezuka, Y. et al. (2016). Topological "interfacial" polymer chemistry: dependency of polymer "shape" on surface morphology and stability of layer structures when heating organized molecular films of cyclic and linear block copolymers of n-butyl acrylate-ethylene oxide. *J. Polym. Sci., Part B: Polym. Phys.* 54: 486–498. https://doi.org/10.1002/polb.23936.

26 Schmidt, I. and Binder, K. (1985). Model calculations for wetting transitions in polymer mixtures. *J. Phys.* 46: 1631–1644. https://doi.org/10.1051/jphys:0198500460100163100.

27 Nakanishi, H. and Pincus, P. (1983). Surface spinodals and extended wetting in fluids and polymer solutions. *J. Chem. Phys.* 79: 997–1003. https://doi.org/10.1063/1.445880.

28 Fowkes, F.M. (1965). Attractive forces at interfaces. In: *Chemistry and Physics at Interfaces*, vol. 1 (ed. S. Ross), 1–12. American Chemical Society.

29 Braught, D.C., Bruning, D.D., and Scholz, J.J. (1969). Adsorption of rare gases on poly(vinyl chloride). *J. Colloid Interface Sci.* 31: 263–269.

30 Ruckenstein, E. and Gourisankar, S.V. (1986). Surface restructuring of polymeric solids and its effect on the stability of the polymer–water interface. *J. Colloid Interface Sci.* 109: 557–566. https://doi.org/10.1016/0021-9797(86)90337-1.

31 Chen, J., Zhuang, H., Zhao, J., and Gardella, J.A. (2001). Solvent effects on polymer surface structure. *Surf. Interface Anal.* 31: 713–720. https://doi.org/10.1002/sia.1097.

32 Lohr, J.E. and Scholz, J.J. (1965). Physical adsorption on poly(methyl methacrylate). *J. Colloid Sci.* 20: 846–856.

33 Hoburg, R.F., Handler, G.S., and Scholz, J.J. (1968). Adsorption studies on polystyrene. *J. Colloid Interface Sci.* 27: 642–648. https://doi.org/10.1016/0021-9797(68)90096-9.

34 Ninham, B.W. and Yaminsky, V. (1997). Ion binding and ion specificity: the Hofmeister effect and Onsager and Lifshitz theories. *Langmuir* 13: 2097–2108. https://doi.org/10.1021/la960974y.

35 Jacobasch, H.J., Simon, F., and Weidenhammer, P. (1998). Adsorption of ions onto polymer surfaces and its influence on zeta potential and adhesion phenomena. *Colloid. Polym. Sci.* 276: 434–442. https://doi.org/10.1007/s003960050263.

36 Sidorenko, A., Minko, S., Schenk-Meuser, K. et al. (1999). Switching of polymer brushes. *Langmuir* 15: 8349–8355. https://doi.org/10.1021/la990869z.

37 Thomas, H.R. and O'Malley, J.J. (1979). Surface studies on multicomponent polymer systems by X-ray photoelection spectroscopy. Polystyrene/poly(ethylene oxide) diblock copolymers. *Macromolecules* 12: 323–329. https://doi.org/10.1021/ma60068a033.

38 Veith, C.A., Cohen, R.E., and Argon, A.S. (1991). Morphologies of poly(dimethylsiloxane)-nylon-6 diblock copolymers and blends. *Polymer (Guildf)* 32: 1545–1554.

39 Barton, A.F.M. (1990). *Handbook of Polymer-Liquid Interaction Parameters and Solubility Parameters*. CRC Press.

40 Horn, R.G. (1990). Surface forces and their actions in ceramic materials. *J. Am. Ceram. Soc.* 73: 1117–1135. https://doi.org/10.1111/j.1151-2916.1990.tb05168.x.

41 Jones, D.M., Smith, J.R., Huck, W.T.S., and Alexander, C. (2002). Variable adhesion of micropatterned thermoresponsive polymer brushes: AFM investigations of poly(*N*-isopropylacrylamide) brushes prepared by surface-initiated polymerizations. *Adv. Mater.* 14: 1130–1134.

42 Spruijt, E., Choi, E.Y., and Huck, W.T.S. (2008). Reversible electrochemical switching of polyelectrolyte brush surface energy using electroactive counterions. *Langmuir* 24: 11253–11260. https://doi.org/10.1021/la801994b.

43 Li, J.J., Zhou, Y.N., and Luo, Z.H. (2014). Thermo-responsive brush copolymers with structure-tunable LCST and switchable surface wettability. *Polymer (Guildf)* 55: 6552–6560. https://doi.org/10.1016/j.polymer.2014.10.025.

44 Merlitz, H., He, G.L., Sommer, J.U., and Wu, C.X. (2009). Reversibly switchable polymer brushes with hydrophobic/hydrophilic behavior: a langevin dynamics study. *Macromolecules* 42: 445–451. https://doi.org/10.1021/ma8019877.

45 Cui, W., Su, C.F., Merlitz, H. et al. (2014). Structure of dendrimer brushes: mean-field theory and MD simulations. *Macromolecules* 47: 3645–3653. https://doi.org/10.1021/ma500129h.

46 De Beer, S. (2014). Switchable friction using contacts of stimulus-responsive and nonresponding swollen polymer brushes. *Langmuir* 30: 8085–8090. https://doi.org/10.1021/la5013473.

47 Sariban, A., Binder, K., Sariban, A., and Binder, K. (2017). Critical properties of the Flory – Huggins lattice model of polymer mixtures. *J. Chem. Phys.* 86: 5859–5873. https://doi.org/10.1063/1.452516.

48 Bates, F.S., Rosedale, J.H., Stepanek, P. et al. (1990). Static and dynamic crossover in a critical polymer mixture. *Phys. Rev. Lett.* 65: 1893–1896.

49 Flory, P.J., Orwoll, R.A., and Vrij, A. (1964). Statistical thermodynamics of chain molecule liquids. II. Liquid mixtures of normal paraffin hydrocarbons. *J. Am. Chem. Soc.* 86: 3515–3520.

50 Jalbert, C. and Koberstein, J.T. (1997). End group effects on surface properties of polymers: semiempirical calculations and comparison to experimental surface tensions for α,ω-functional poly(dimethylsiloxanes). *Macromolecules* 30: 4481–4490.

51 O'Rourke Muisener, P.A.V., Jalbert, C.A., Yuan, C. et al. (2003). Measurement and modeling of end group concentration depth profiles for ω-fluorosilane polystyrene and its blends. *Macromolecules* 36: 2956–2966.

52 Shibayama, M., Yang, X., Stein, R.S., and Han, C.C. (1985). Study of miscibility and critical phenomena of deuterated polystyrene and hydrogenated poly(vinyl methyl ether) by small-angle neutron scattering. *Macromolecules* 19: 2179–2187.

53 Smerdova, O., Graham, R.S., Gasser, U. et al. (2014). A novel method of extraction of blend component structure from sans measurements of homopolymer bimodal blends. *Macromol. Chem. Phys.* 215: 859–866. https://doi.org/10.1002/macp.201300787.

54 Seul, M., Morgan, N.Y., and Sire, C. (1994). Domain coarsening in a two-dimensional binary mixture: growth dynamics and spatial correlations. *Phys. Rev. Lett.* 73: 2284–2287. https://doi.org/10.1103/PhysRevLett.73.2284.

55 Rigoussen, A., Verge, P., Raquez, J. et al. (2017). In-depth investigation on the effect and role of cardanol in the compatibilization of PLA/ABS immiscible blends by reactive extrusion. *Eur. Polym. J.* 93: 272–283. https://doi.org/10.1016/j.eurpolymj.2017.06.004.

56 Rigoussen, A., Verge, P., Raquez, J., and Dubois, P. (2018). Natural phenolic antioxidants as a source of bio-compatibilizers for immiscible polymer blends. *ACS Sustainable Chem. Eng.* https://doi.org/10.1021/acssuschemeng.8b02999.

57 Raquez, J., Degée, P., Nabar, Y., and Narayan, R. (2006). Biodegradable materials by reactive extrusion: from catalyzed polymerization to functionalization and blend compatibilization. *C.R. Chim.* 9: 1370–1379. https://doi.org/10.1016/j.crci.2006.09.004.

58 Raquez, J., Narayan, R., and Dubois, P. (2008). Recent advances in reactive extrusion processing of biodegradable polymer-based compositions. *Macromol. Mater. Eng.* 293: 447–470. https://doi.org/10.1002/mame.200700395.

59 Zhao, F., Wang, C., and Zhan, X. (2018). Morphology control in organic solar cells. *Adv. Energy Mater.* 1703147, 1–34. https://doi.org/10.1002/aenm.201703147.

60 Nadgorny, M. and Ameli, A. (2018). Functional polymers and nanocomposites for 3D printing of smart structures and devices. *ACS Appl. Mater. Interfaces* 10: 17489–17507. https://doi.org/10.1021/acsami.8b01786.

61 Naveed, H.B. and Ma, W. (2018). Miscibility-driven optimization of nanostructures in ternary organic solar cells using non-fullerene acceptors. *Joule*: 1–21. https://doi.org/10.1016/j.joule.2018.02.010.

62 Li, Q., Yao, F., Liu, Y. et al. (2018). High-temperature dielectric materials for electrical energy storage. *Annu. Rev. Mater. Res.* 48: 1–25.

63 Zhang, B., Sudre, G., Quintard, G. et al. (2017). Guar gum as biosourced building block to generate highly conductive and elastic ionogels with poly(ionic liquid) and ionic liquid. *Carbohydr. Polym.* 157: 586–595. https://doi.org/10.1016/j.carbpol.2016.10.050.

64 Padil, V.V.T., Miroslav, Č., and Varma, R.S. (2018). Tree gum-based renewable materials: sustainable applications in nanotechnology, biomedical and environmental fields. *Biotechnol. Adv.* 36: 1984–2016. https://doi.org/10.1016/j.biotechadv.2018.08.008.

65 Mari, M. (2018). How green is your plasticizer? *Polymers* 10: 1–17. https://doi.org/10.3390/polym10080834.

66 Persenaire, O., Quintana, R., Lemmouchi, Y. et al. (2014). Reactive compatibilization of poly(L-lactide)/poly(butylene succinate) blends through polyester maleation: from materials to properties. *Polym. Int.* 63: 1724–1731. https://doi.org/10.1002/pi.4700.

67 Persenaire, O., Raquez, J., and Dubois, P. (2010). Tailoring of co-continuous polymer blend morphology: joint action of nanoclays and compatibilizers. *Macromol. Chem. Phys.* 211: 1433–1440. https://doi.org/10.1002/macp.200900704.

68 Quintana, R., Persenaire, O., Lemmouchi, Y. et al. (2016). Compatibilization of co-plasticized cellulose acetate/water soluble polymers blends by reactive extrusion. *Polym. Degrad. Stab.* 126: 31–38. https://doi.org/10.1016/j.polymdegradstab.2015.12.023.

69 Quintana, R., Persenaire, O., Lemmouchi, Y. et al. (2014). Grafted D/L-lactide to cellulose acetate by reactive melt processing: its role as CA/PLA blend compatibilizer. *Eur. Polym. J.* 57: 30–36. https://doi.org/10.1016/j.eurpolymj.2014.05.003.

70 Mincheva, R., Jasmani, L., Josse, T. et al. (2016). Binary mixed homopolymer brushes tethered to cellulose nanocrystals: a step towards compatibilized polyester blends. *Biomacromolecules* 9 https://doi.org/10.1021/acs.biomac.6b00932.

71 Barrau, S., Lefebvre, J., Raquez, J., and Dubois, P. (2014). Designing multiple-shape memory polymers with miscible polymer blends: evidence and origins of a triple-shape memory effect for miscible PLLA/PMMA blends. *Macromolecules* 47: 6791–6803.

72 Samuel, C., Raquez, J., and Dubois, P. (2016). Biobased poly(lactides)/poly(methyl methacrylate) blends: a perfect association for durable and smart applications? *AIP Conf. Proc.* 030005, 1–5. https://doi.org/10.1063/1.4918395.

73 Samuel, C., Raquez, J., and Dubois, P. (2013). PLLA/PMMA blends: a shear-induced miscibility with tunable morphologies and properties? *Polymer (Guildf)* 54: 3931–3939. https://doi.org/10.1016/j.polymer.2013.05.021.

74 Walls, J.D., Nur, A.M., and Bourbie, T. (1982). Effects of pressure and partial water saturation on gas permeability in tight sands: experimental results. *J. Pet. Technol.* 34: 930–936. https://doi.org/10.1016/0148-9062(83)91680-7.

75 Schell, W.J. (1985). Commercial applications for gas permeation membrane systems. *J. Membr. Sci.* 22: 217–224. https://doi.org/10.1016/S0376-7388(00)81281-8.

76 Ruthven, D.M. (1984). *Principles of Adsorption and Adsorption Processes.* USA: Wiley (A Wiley Interscience Publication).

77 Hunter, C.A. and Sanders, J.K.M. (1990). The nature of π–π interactions. *J. Am. Chem. Soc.* 112: 5525–5534.

78 Sugimoto, S., Inutsuka, M., Kawaguchi, D., and Tanaka, K. (2018). Reorientation kinetics of local conformation of polyisoprene at substrate interface. *ACS Macro Lett.* 7: 85–89. https://doi.org/10.1021/acsmacrolett.7b00927.

79 Nguyen, H.K., Inutsuka, M., Kawaguchi, D., and Tanaka, K. (2018). Direct observation of conformational relaxation of polymer chains at surfaces. *ACS Macro Lett.* 7: 1198–1202. https://doi.org/10.1021/acsmacrolett.8b00411.

80 Inutsuka, M., Horinouchi, A., and Tanaka, K. (2015). Aggregation states of polymers at hydrophobic and hydrophilic solid interfaces. *ACS Macro Lett.* 4: 1174–1178. https://doi.org/10.1021/acsmacrolett.5b00592.

81 Chen, Z. (2010). Investigating buried polymer interfaces using sum frequency generation vibrational spectroscopy. *Prog. Polym. Sci.* 35: 1376–1402. https://doi.org/10.1016/j.progpolymsci.2010.07.003.

82 Lu, X., Shephard, N., Han, J. et al. (2008). Probing molecular structures of polymer/metal interfaces by sum frequency generation vibrational spectroscopy. *Macromolecules* 41: 8770–8777. https://doi.org/10.1021/ma801680f.

83 Lu, X., Xue, G., Wang, X. et al. (2012). Directly probing molecular ordering at the buried polymer/metal interface 2: using P-polarized input beams. *Macromolecules* 45: 6087–6094. https://doi.org/10.1021/ma301088g.

84 Lu, X., Myers, J.N., and Chen, Z. (2014). Molecular ordering of phenyl groups at the buried polystyrene/metal interface. *Langmuir* 30: 9418–9422. https://doi.org/10.1021/la502037h.

85 Fang, Y., Li, B., Yu, J. et al. (2013). Probing surface and interfacial molecular structures of a rubbery adhesion promoter using sum frequency generation vibrational spectroscopy. *Surf. Sci.* 615: 26–32. https://doi.org/10.1016/j.susc.2013.04.013.

86 Yagi, I., Inokuma, K., Kimijima, K., and Notsu, H. (2014). Molecular structure of buried perfluorosulfonated ionomer/Pt interface probed by vibrational sum frequency generation spectroscopy. *J. Phys. Chem. C* 118: 26182–26190.

87 Tsuruta, H., Fujii, Y., Kai, N. et al. (2012). Local conformation and relaxation of polystyrene at substrate interface. *Macromolecules* 45: 4643–4649. https://doi.org/10.1021/ma3007202.

88 Wilson, P.T., Richter, L.J., Wallace, W.E. et al. (2002). Correlation of molecular orientation with adhesion at polystyrene/solid interfaces. *Chem. Phys. Lett.* 363: 161–168. https://doi.org/10.1016/S0009-2614(02)01171-5.

89 Silberberg, A. (1982). Distribution of conformations and chain ends near the surface of a melt of linear flexible macromolecules. *J. Colloid Interface Sci.* 90: 86–91. https://doi.org/10.1016/0021-9797(82)90400-3.

90 Bitsanis, I.A. and Ten Brinke, G. (1993). A lattice Monte Carlo study of long chain conformations at solid-polymer melt interfaces. *J. Chem. Phys.* 99: 3100–3111. https://doi.org/10.1063/1.465163.

91 Firkowska-Boden, I., Zhang, X., and Jandt, K.D. (2018). Controlling protein adsorption through nanostructured polymeric surfaces. *Adv. Healthc. Mater.* 7: 1–19. https://doi.org/10.1002/adhm.201700995.

92 Dragneva, N., Rubel, O., and Floriano, W.B. (2016). Molecular dynamics of fibrinogen adsorption onto graphene, but not onto poly(ethylene glycol) surface, increases exposure of recognition sites that trigger immune response. *J. Chem. Inf. Model.* 56: 706–720. https://doi.org/10.1021/acs.jcim.5b00703.

93 Tang, L., Ugarova, T.P., Plow, E.F., and Eaton, J.W. (1996). Molecular determinants of acute inflammatory responses to biomaterials. *J. Clin. Invest.* 97: 1329–1334. https://doi.org/10.1172/JCI118549.

94 Roach, P., Farrar, D., and Perry, C.C. (2005). Interpretation of protein adsorption: surface-induced conformational changes. *J. Am. Chem. Soc.* 127: 8168–8173.

95 Zhang, X., Helbing, C., Arras, M.M.L. et al. (2017). Nanocrystal width controls fibrinogen orientation and assembly kinetics on poly(butene-1) surfaces. *Langmuir* 33: 6563–6571. https://doi.org/10.1021/acs.langmuir.7b01365.

96 Roach, P., Farrar, D., and Perry, C.C. (2006). Surface tailoring for controlled protein adsorption: effect of topography at the nanometer scale and chemistry. *J. Am. Chem. Soc.* 128: 3939–3945.

97 Giamblanco, N., Martines, E., and Marletta, G. (2013). Laminin adsorption on nanostructures: switching the molecular orientation by local curvature changes. *Langmuir* 29: 8335–8342. https://doi.org/10.1021/la304644z.

98 Hammarin, G., Persson, H., Dabkowska, A.P., and Prinz, C.N. (2014). Enhanced laminin adsorption on nanowires compared to flat surfaces. *Colloids Surf., B* 122: 85–89. https://doi.org/10.1016/j.colsurfb.2014.06.048.

99 Fortes, M.A. (1983). *Physicochemical Aspects of Polymer Surfaces*. Hopewell Junction, NY: IBM Corporation.

100 Young, T. (1804). An essay on the cohesion of fluids. *Philos. Trans. R. Soc. London* 95: 65–87.

101 Eral, H.B., Mannetje, D.J.C.M., and Oh, J.M. (2013). Contact angle hysteresis: a review of fundamentals and applications. *Colloid. Polym. Sci.* 291: 247–260. https://doi.org/10.1007/s00396-012-2796-6.

102 Beigbeder, A., Mincheva, R., Pettitt, M.E. et al. (2010). Marine fouling release silicone/carbon nanotube nanocomposite coatings: on the importance of the nanotube dispersion state. *J. Nanosci. Nanotechnol.* 10: 2972–2978. https://doi.org/10.1166/jnn.2010.2185.

103 Tanaka, K., Takahara, A., and Kajiyama, T. (1995). Surface molecular motion in thin films of poly(styrene-block-methyl methacrylate) diblock copolymer. *Acta Polym.* 46: 476–482. https://doi.org/10.1002/actp.1995.010460612.

104 Chrissopoulou, K. and Anastasiadis, S.H. (2015). Effects of nanoscopic-confinement on polymer dynamics. *Soft Matter* 11: 3746–3766. https://doi.org/10.1039/c5sm00554j.

105 Fox, T.G. and Loshaek, S. (1955). Influence of molecular weight and degree of crosslinking on the specific volume and glass temperature of polymers. *J. Polym. Sci.* 15: 371–390. https://doi.org/10.1002/pol.1955.120158006.

106 Fox, T.G. (1956). Influence of diluent and of copolymer composition on the glass temperature of a polymer system. *Bull. Am. Phys. Soc.* 57: 1259–1272. https://doi.org/10.1002/prca.201200064.

107 Mischler, C., Baschnagel, J., and Binder, K. (2001). Polymer films in the normal-liquid and supercooled state: a review of recent Monte Carlo simulation results. *Adv. Colloid Interface Sci.* 94: 197–227. https://doi.org/10.1016/S0001-8686(01)00061-6.

108 Keller, A. and Cheng, S.Z.D. (1998). The role of metastability in polymer phase transitions. *Polymer (Guildf)* 39: 4461–4487. https://doi.org/10.1016/S0032-3861(97)10320-2.

109 Hobbs, J.K., Farrance, O.E., and Kailas, L. (2009). How atomic force microscopy has contributed to our understanding of polymer crystallization. *Polymer (Guildf)* 50: 4281–4292. https://doi.org/10.1016/j.polymer.2009.06.021.

110 Olmsted, P.D., Poon, W.C.K., McLeish, T.C.B. et al. (1998). Spinodal-assisted crystallization in polymer melts. *Phys. Rev. Lett.* 81: 373–376. https://doi.org/10.1103/PhysRevLett.81.373.

111 Durell, M., Macdonald, J.E., Trolley, D. et al. (2002). The role of surface-induced ordering in the crystallisation of PET films. *Europhys. Lett.* 58: 844–850. https://doi.org/10.1209/epl/i2002-00451-1.

112 Jukes, P.C., Das, A., Durell, M. et al. (2005). Kinetics of surface crystallization in thin films of poly(ethylene terephthalate). *Macromolecules* 38: 2315–2320. https://doi.org/10.1021/ma0490606.

113 Kei Shinotsuka, H.E.A. and Bliznyuk, V.N. (2012). Near-surface crystallization of PET. *Polymer (Guildf)* 53: 5554–5559. https://doi.org/10.1016/j.polymer.2012.09.048.

114 Yasuda, K., Kim, A., Cho, H. et al. (2016). Specular reflection from rough surfaces revisited. *Phys. Teach.* 54: 394–396. https://doi.org/10.1119/1.4962772.

115 Kajiyama, T., Tanaka, K., Ge, S.R., and Takahara, A. (1996). Morphology and mechanical properties of polymer surfaces via scanning force microscopy. *Prog. Surf. Sci.* 52: 1–52. https://doi.org/10.1016/0079-6816(96)00006-8.

116 Coulon, G. (2000). Imagerie de surface de polymères: microscopie à force atomique. *J. Mol. Biol.* AM/01: AM3280.

117 Hochstetter, G., Jimenez, A., and Loubet, J.L. (1999). Strain-rate effects on hardness of glassy polymers in the nanoscale range. Comparison between quasi-static and continuous stiffness measurements. *J. Macromol. Sci. Part B* 38: 681–692. https://doi.org/10.1080/00222349908248131.

118 Felder, E., Bucaille, J.L., and Hochstetter, G. (2003). Influence de la rheologie des polymeres sur leur resistance a la rayure: etude experimentale et par simulation numerique. *Ann. Chim. Sci. Des Mater.* 28: 15–28. https://doi.org/10.1016/S0151-9107(03)00049-7.

119 Nagel, W.E., Kröner, D.H., and Resch, M.M. (2017). *High Performance Computing in Science and Engineering '17*. Transactions of the High Performance Computing Center, Stuttgart (HLRS). ISBN: 978-3-319-68394-2.